Electronic effects of alloying elements Nb and V on body-centred-cubic Fe grain boundary cohesion

Jia-Xiang Shang[1] **and Chong-Yu Wang**[1,2,3]

[1] Central Iron and Steel Research Institute, Beijing 100081, China
[2] Department of Physics, Tsinghua University, Beijing 100084, China
[3] International Centre for Materials Physics, Academia Sinica, Shenyang 110016, China

Abstract
The segregation effects of Nb and V on bcc $Fe\Sigma3[1\bar{1}0](111)$ grain boundary cohesion are studied by the first-principles DMol method within the framework of density functional theory. The calculated segregation energy difference between the grain boundary and the corresponding free surface is -0.51 eV (-0.58 eV) for solute Nb (V), which indicates that both Nb and V could enhance the grain boundary cohesion in body-centred-cubic Fe. We found that the chemical effect and the geometry effect of Nb (V) play crucial but opposite roles in determining whether a material is brittle or ductile. The chemical effect is dominant and advantageous for grain boundary cohesion. Also, Nb and V show very different behaviours: in chemical effect, Nb is more conducive to ductility than V; while in the geometry effect, Nb is less conducive to ductility and more conducive to embrittlement than V.

1. Introduction

Due to its low price and excellent mechanical properties, steel is one of the most important and widely used metallic materials. It is well known that the intergranular segregation effects of alloying elements such as Si, Mn, Nb, Mo, V and Ti play important roles in determining the cohesion properties of Fe grain boundaries (GB), and will further affect the two key mechanical properties: strength and toughness in structural steels. The different segregated elements may have different effects on the intergranular fracture. So the selections of alloying element and processing technology are crucial for obtaining good mechanical properties. Microalloying has a strong effect on grain refinement; this forms the basis of an approach used to increase the strength and improve the toughness of steel materials. Obviously, the segregation of an alloying element on a GB will cause a change of the atomic microstructure and electronic structure of the GB, and further affect the mechanical properties of the material. So the study of the intergranular segregation effect of the alloying element has great significance for understanding the mechanical properties of steel materials.

On the basis of Griffith fracture theory [1], Rice and Wang [2] have presented a thermo-dynamic model for describing the mechanism of impurity-induced embrittlement through the competition between plastic crack blunting by dislocation emission and brittle boundary separation. In their model, the relationship between the cleavage works with ($2\gamma_{int}$) and without ($2\gamma_{int}^0$) a solute atom is expressed approximately as

$$2\gamma_{int} = 2\gamma_{int}^0 - (\Delta E_{GB} - \Delta E_{FS})\Gamma$$

where Γ is the solute coverage of impurity, and ΔE_{GB} and ΔE_{FS} are the impurity segregation energies at the GB and at the free surface (FS) respectively. One can predict whether the solute atom enhances or weakens the GB cohesion from the sign of $\Delta E_{GB} - \Delta E_{FS}$. It can be concluded that: (1) if the sign is minus, the solute atom will be easy to segregate on a GB and will enhance the GB cohesion; while (2) if it is plus, the solute atom will prefer to segregate on a FS and thus will be disadvantageous to GB cohesion. Experimental investigation of steels containing H, B, Sn, Sb and S has provided support for the above descriptions [2].

In the past decade, on the basis of the Rice–Wang model, some researchers have made theoretical efforts to understand the segregation effect of light impurities such as B, C, P and S, and 3d transition elements such as Cr and Mn on Fe GB cohesion by making first-principles calculations [3–12]. They obtained some exciting results which are in good agreement with experiment and have been used in materials design. These studies showed that it may be beneficial to consider the electronic effect in the study of steel materials, in order to achieve considerable insight into the mechanical properties of such materials.

From the Rice–Wang model mentioned above, we know that ΔE_{GB} and ΔE_{FS} are the two dominant quantities in brittle/ductile determination for solute atoms and can be determined accurately by first-principles calculation. In the present work, we have adopted the first-principles DMol method [13, 14] to investigate the segregation effects of two important alloying elements, Nb and V, on bcc FeΣ3[1$\bar{1}$0](111) GB cohesion. We present the computation method and cluster model in section 2, and give the results and a discussion in sections 3, 4 and 5. The last section is a summary.

2. Computational method and cluster model

The DMol method is a first-principles numerical method within the framework of density functional theory [15, 16]. One of its merits is that it includes an energy gradient calculation, from which one can obtain the desired optimized atomic structure. This is important in the case of study of local problems such as the effects of element doping on the GB and FS, where the new element will usually cause a local distortion of other atomic sites around it. The cluster models used in the present DMol calculation are shown in figure 1. Figure 1(a) and figure 1(b) present the atomic structures of the FeΣ3[1$\bar{1}$0](111) GB (including 71 atoms) and the Fe(111) FS (including 58 atoms) respectively. The squares and circles represent different Fe layers along the [110] direction. Some atoms in the cluster are labelled with numbers used for discussing the results more clearly. For the larger atomic structure, Nb and V will most probably occupy the substitution site rather than the interstitial site on the GB or FS. In this work, we just consider the substitution case, and the Nb (V) atom is assigned as substituting for the Fe1 atom. Naturally, an Nb (V) atom will induce local stress around it. Considering the interaction between Nb (V) and the nearest-neighbouring Fe atom is the most important; we use the DMol method to relax just the first-shell Fe atoms around the Nb (V) atom to release the stress. The numbers of relaxed atoms in the GB model and in the FS model are 15 and 8 respectively. The relaxed atoms are labelled in figure 1.
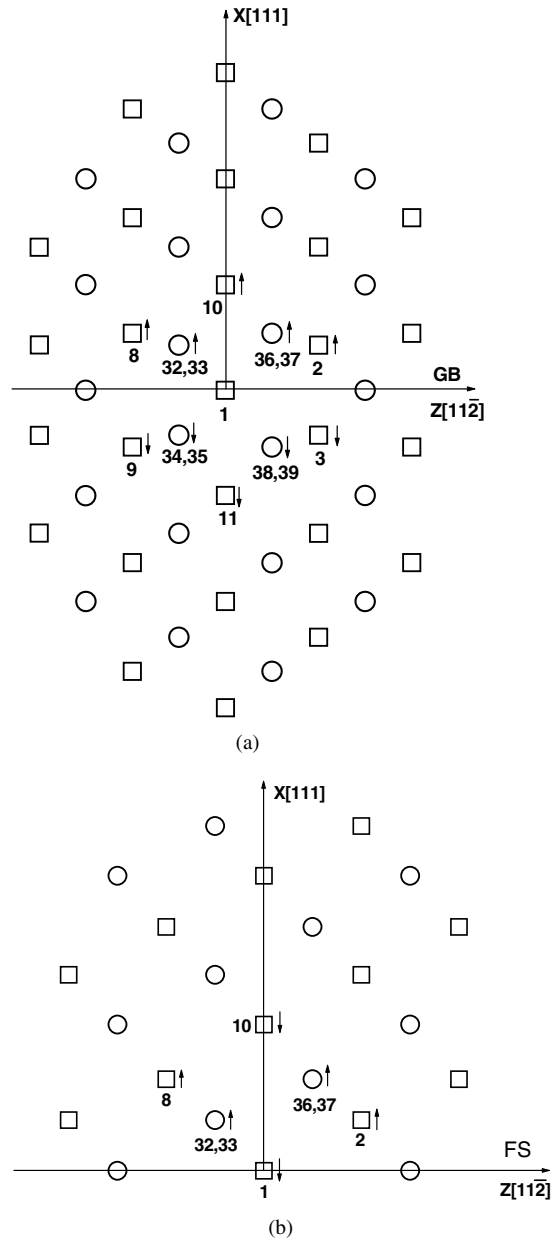
Figure 1. The atomic structure of cluster models for (a) the Fe$\Sigma 3[1\bar{1}0](111)$ GB (the $X = 0$ plane is the GB plane); (b) the Fe(111) FS. The squares and circles represent Fe atoms in different Fe layers along the [110] direction respectively. Atoms labelled with numbers are atoms relaxed in the DMol calculation. The arrow displays the direction of atomic movement after DMol relaxation. The square labelled number 1 is the substitution site for Nb (V) in the GB and FS.

The DMol method provides various types of basis set; the double numerical basis with polarized functions (DNP) was proved to be able to yield the most reliable result. In this work, we adopted the DNP as the basis set. The orbitals beyond 3s (4s) were taken as the self-consistent valence orbitals and those below 3s (4s) were taken as the core orbitals for

Fe and V (Nb) atoms. The valence orbitals were further refined by the usual valence–core orbital orthogonalization technique and the core effect was considered via the charge density. The Vosko–Wilk–Nusair local spin-exchange correlation potential [17] was employed. The binding energy of the cluster system is defined as the difference of the total energy of the interacting atom system from that of the free-atom system. We obtained the optimized atomic structure and the binding energy of the system from the energy gradient on the relaxed atom converged to 0.001 eV Å^{-1}.

3. The effects of Nb (V) on the atomic structure of the GB and FS

In this study, the original atomic configuration of the bcc FeΣ3[1$\bar{1}$0](111) GB was constructed by use of the coincidence site lattice (CSL) model, which consists of 2562 atoms. The ideal (111) FS including 1300 atoms is also constructed. The CSL models of GB and ideal FS may not be stable. For this reason, we performed the long-range molecular dynamics [18] (MD) optimization with the Finnis–Sinclair potential [19, 20] on the CSL GB and FS configurations. The total energies of the systems decreased by 12.81 eV for the GB and 2.56 eV for the FS respectively. The optimized GB and FS configurations are in agreement with another group's MD result [21].

The cluster models of the Fe GB and FS for the DMol calculation as shown in figure 1 are generated from the MD results. We know that the long-range MD relaxation is sometimes insufficient for dealing with the defect system. So we performed DMol relaxations on the Fe GB and FS systems obtained by means of MD first, and the results are identified as those for 'clean GB' and 'clean FS' systems. Then we performed similar DMol relaxations on Fe GB and FS systems where the Fe1 atom is replaced by a Nb (V) atom, and the results are identified as those for 'Nb- (V-) doped GB' and 'Nb- (V-) doped FS' systems.

We found that the movements of relaxed atoms in Nb- (V-) doped GB and Nb- (V-) doped FS systems are mainly along [111] directions (as shown in figure 1), and those along other directions are almost unchanged. The displacement of the relaxed atomic position along the [111] direction in the Nb- (V-) doped system relative to that in the clean system is given in table 1. For the Nb-doped GB system, we can see that the Fe atoms close to Nb are pushed away from the GB plane to different degrees. Fe10, Fe8 and Fe2 atoms which are in the same (110) plane as the Nb show relatively large displacements; in particular, Fe10 has the largest displacement, of 0.144 Å. However, for the V-doped GB system, the positions of these Fe atoms are hardly affected. This may be attributed to the atomic size of V being smaller than that of Nb. For the Nb- (V-) doped FS system, the Nb (V) atom moves along [111] in the opposite direction to its movement on the outside of the FS, and, unlike in the case for

Table 1. The atomic displacement (in Å) along the [111] direction caused by DMol relaxation in the GB and FS.

	Nb-doped		V-doped	
	GB	FS	GB	FS
Nb (V)	0.000	−0.360	0.000	−0.088
Fe2	0.056	0.022	0.000	0.041
Fe8	0.070	0.017	0.000	0.038
Fe10	0.144	−0.240	0.000	−0.243
Fe32	0.024	0.061	0.000	0.037
Fe36	0.066	0.061	0.000	0.047

the Nb- (V-) doped GB, Fe10 also moves along [111] in the opposite direction, to reduce the system energy. The other Fe atoms, such as Fe2 and Fe8, still move along the [111] direction. We also find that for the doped FS system, the displacements of the Fe atoms which are in the same (110) plane as the V are larger than those for atoms in the same plane as the Nb, while the case is just the opposite for Fe atoms in other (110) planes. Comparing with the results on GB (FS) doped with light impurities, B (C, S, P), studied by other groups [6–8], we find that Nb has a similar effect to B (C, P, S) on the atomic structure of $Fe\Sigma 3[1\bar{1}0](111)$ GB: Nb will make the neighbouring Fe atoms expand outside the GB plane. However, Nb (V) shows different movement behaviour to B (C, P, S) on the FS: it will move to the outside of the FS. These effects are advantageous to the binding of Fe atoms which are on the inside of the interface (surface), while the GB cohesion will be mainly compensated by the interaction of Nb (V) with Fe. This can be seen in the next section's discussion.

4. Segregation energy

The segregation energy is defined as the binding energy difference between the doped system and the clean system. The results for doped GB and doped FS are given in table 2. According to the Rice–Wang model, we can conclude that both Nb and V are enhancers and could enhance the bcc $Fe\Sigma 3$ GB cohesion, because the calculated differences in segregation energy between the GB and FS are -0.51 eV and -0.58 eV for solutes Nb and V respectively. The study by Yang *et al* [12] showed that Cr acts as a cohesion enhancer and Mn is an embrittler in fcc Fe GB.

Table 2. Segregation energies (in eV) of Nb/Fe and V/Fe systems.

		ΔE_{GB}	ΔE_{FS}	$\Delta E_{GB} - \Delta E_{FS}$
Nb/Fe	Chemical effect	-2.84	-1.89	-0.95
	Geometry effect	-0.27	-0.71	0.44
	Total	-3.11	-2.60	-0.51
V/Fe	Chemical effect	-2.59	-1.84	-0.75
	Geometry effect	0.00	-0.17	0.17
	Total	-2.59	-2.01	-0.58

We know that the binding energy is comprised primarily of two parts which are induced by the chemical effect and geometry effect respectively. To obtain a good understanding of the nature of the mechanism determining whether a material is brittle or ductile upon substitution of Nb (V), it may be useful to clarify the roles of the chemical effect and geometry effect in the segregation behaviour separately. The chemical effect refers to the effect induced by substitution of Nb (V) for Fe1, without considering structure relaxation. However, in the geometry effect, only the structure relaxation contribution is considered. The contributions from the two effects to the segregation energy are summarized in table 2. It can be seen that the chemical effect of Nb (V) plays a major role in determining whether a material is brittle or ductile, and favours GB cohesion. Nb has a stronger chemical effect than V as regards GB cohesion. In contrast, the geometry effect of Nb (V) contributes a positive value of $\Delta E_{GB} - \Delta E_{FS}$, and thus does not favour GB cohesion. We can see that Nb is more conducive to embrittlement than V in its geometry effect. The results suggest that the local distortion induced by Nb (V) plays an important role in determining whether a material is brittle or ductile also, and cannot be neglected. So DMol optimization is necessary in the computation.

5. Charge distribution, magnetism and local density of states

In this section, we discuss the results on the charge distribution, magnetism and local density of states (LDOS) for the Nb- (V-) doped GB system only.

The charge-density difference is obtained from

$$\Delta\rho = [\rho(\text{Nb- (V-) doped GB}) - \rho(\text{clean GB})] - [\rho(\text{Nb (V)}) - \rho(\text{Fe1})]$$

where $\rho(\text{Nb- (V-) doped GB})$, $\rho(\text{clean GB})$, $\rho(\text{Nb (V)})$ and $\rho(\text{Fe1})$ are the charge densities of the Nb- (V-) doped GB, clean GB, free Nb (V) atom and free Fe1 atom respectively. The charge-density differences on the (110) plane for Nb-doped GB and V-doped GB are shown in figure 2. Figure 2 shows clearly the enhanced atom bondings of Fe2 with Fe3 and Fe8 with Fe9, for a remarkable quantity of electrons accumulate into the regions between these atoms. It is surprising that even though the interatomic distances of Fe2 from Fe3 and Fe8 from Fe9 in Nb-doped GB are larger than those in V-doped GB, the atom bonding of Fe2 with Fe3 and Fe8 with Fe9 in Nb-doped GB are enhanced somewhat more strongly than those in V-doped GB. These effects are mainly attributed to the charge transfer from a doped atom to its neighbouring Fe atoms in Nb-doped GB being different from that in V-doped GB. To show this, we list the electron occupation number data obtained by Mulliken population analysis [22] in table 3. It can be seen that Nb (V) is an electron donor in the GB. Nb contributes more electrons ($0.398e$) to the neighbouring Fe atoms than V ($0.088e$). Most of the electrons which are from Nb
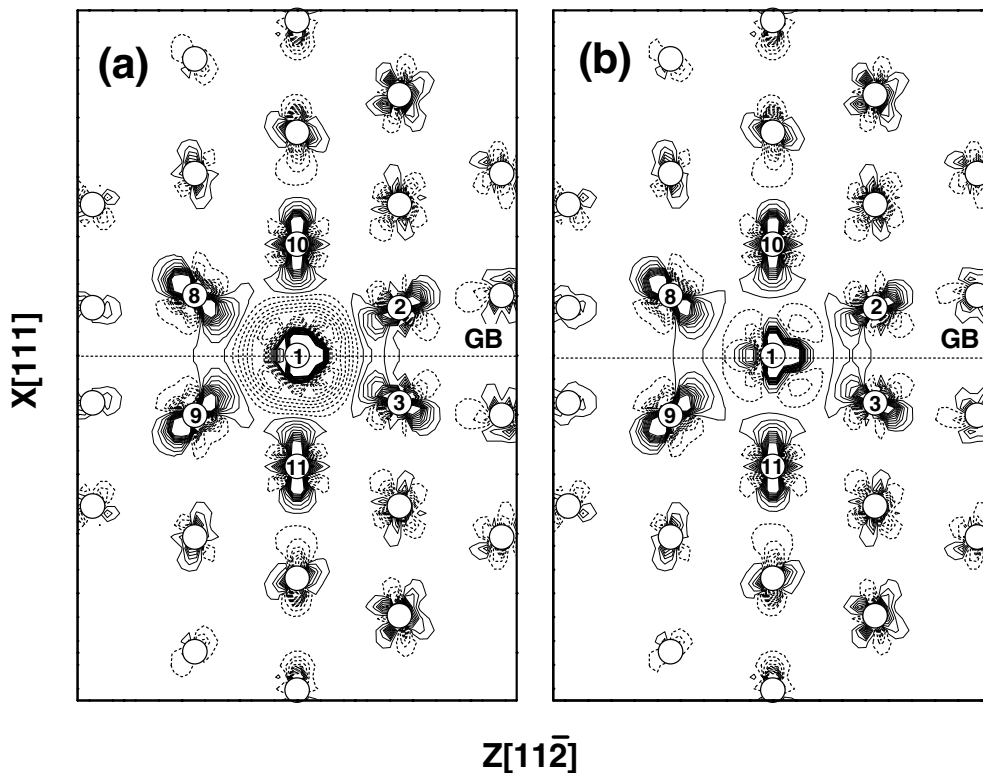
Figure 2. The charge-density difference for $Y = 0$ (110) planes in: (a) Nb-doped GB; (b) V-doped GB. The solid and dashed lines indicate the gain and the loss of electrons respectively. The contour spacing is $0.002\ e\ \text{Å}^{-3}$.

Table 3. The numbers of electrons N_0 (N) occupying valence orbitals and their sum Q for the atom, and the magnetic moments S_0 (S) (in μ_B) in valence orbitals and their sum M for the atom in clean GB (doped GB). For the Fe atom, $\Delta N = N - N_0$, $\Delta Q = Q(\text{doped GB}) - Q(\text{clean GB})$. For the Nb (V) atom, ΔQ is defined as the difference from Q for the free atom.

|		Clean GB		Nb-doped GB				V-doped GB			
		N_0	S_0	N	S	ΔN	ΔQ	N	S	ΔN	ΔQ
Fe1(Nb, V)	3d (4d)	6.854	−1.934	4.144	−0.188			3.863	−0.462		
	4s (5s)	0.556	−0.068	0.151	−0.026			0.431	−0.037		
	4p (5p)	0.629	−0.172	0.307	−0.072			0.618	−0.117		
	Q, M	8.039	−2.174	4.602	−0.286			4.912	−0.616		
Fe2(3)	3d	6.869	−0.638	6.883	−0.518	0.014		6.876	−0.498	0.007	
	4s	0.601	−0.108	0.666	−0.111	0.065		0.609	−0.107	−0.008	
	4p	0.642	−0.295	0.630	−0.315	−0.012		0.640	−0.310	0.002	
	Q, M	8.112	−1.041	8.179	−0.944		0.067	8.125	−0.915		0.013
Fe8(9)	3d	6.852	1.967	6.862	1.754	0.010		6.857	1.631	0.005	
	4s	0.567	0.002	0.612	−0.012	0.045		0.575	−0.011	0.008	
	4p	0.618	−0.086	0.605	−0.117	−0.013		0.616	−0.117	−0.002	
	Q, M	8.036	1.883	8.079	1.625		0.043	8.048	1.503		0.012
Fe32(33–35)	3d	6.870	−1.488	6.884	−0.884	0.014		6.879	−1.092	0.009	
	4s	0.616	−0.097	0.652	−0.079	0.036		0.618	−0.084	0.002	
	4p	0.528	−0.227	0.514	−0.215	−0.014		0.525	−0.223	−0.003	
	Q, M	8.014	−1.812	8.050	−1.178		0.036	8.022	−1.399		0.008
Fe36(37–39)	3d	6.856	2.750	6.872	2.660	0.016		6.867	2.656	0.011	
	4s	0.599	0.051	0.624	0.042	0.025		0.601	0.040	0.002	
	4p	0.494	0.027	0.474	0.005	−0.020		0.489	0.007	−0.005	
	Q, M	7.950	2.828	7.970	2.707		0.020	7.957	2.703		0.007
Fe10(11)	3d	6.867	2.209	6.887	2.039	0.020		6.883	2.092	0.016	
	4s	0.564	−0.004	0.622	−0.028	0.058		0.571	−0.012	0.007	
	4p	0.608	−0.061	0.597	−0.094	−0.011		0.601	−0.080	−0.007	
	Q, M	8.040	2.144	8.106	1.917		0.066	8.055	2.000		0.015

5s, 5p orbitals or V 4s, 4p orbitals accumulate into the regions between Fe atoms, enhancing their bonding. In GB, V 3d orbitals display much stronger abilities to get electrons from the environment than Nb 4d orbitals. These charge-transfer features are reflected distinctly in figure 2 again. We can note that the electron-loss curves around the Nb (V) atom mainly correspond to 5s-like (4s-like) states and that they are denser and more extended in the case of Nb than in that of V. This can be understood from the fundamental electronic properties of 4d and 3d transition metal elements. In fact, the 5s, 5p orbitals of 4d elements are more extended than the 4s, 4p orbitals of 3d elements, and have higher energy states. It is difficult for a 4d element to form directly a stable bonding state with a 3d element. However, the barrier can be removed by the charge-transfer effect, which can cause the 5s, 5p orbitals to be compressed in the host and consequently is favourable to atom bonding. From figure 2, we can also see that the electron-gain curves around the Fe atom are mainly $3d_z$-like features, and those around Nb (V) are s–d mixing features.

It is well known that due to the exchange interaction, bcc Fe will exhibit ferromagnetism at low temperature. However, from table 3, we can see that Fe1, Fe2 and Fe32 atoms form a

spin–antiferromagnetic coupling state with other host Fe atoms in clean GB. The values of the atomic magnetic moments in clean GB are different to those for perfect bcc Fe (about 2.20 μ_B per atom); this results from the different magnitudes of the 3d exchange splitting of Fe atoms in clean GB. For Nb- (V-) doped GB, we can see that the magnetic moments of the neighbouring Fe atoms decrease, which reveals that Nb (V) is a destroyer of magnetism for the host Fe atoms. However, Nb (V) exhibits a small magnetic moment of 0.286 μ_B (0.616 μ_B), and, like the Fe1 atom, forms a spin–antiferromagnetic coupling state with other host Fe atoms also.

The LDOS is obtained by broadening the discrete eigenvalue spectrum with a set of Lorentzian functions. The LDOS curves for some interesting atoms in clean GB, Nb-doped GB and V-doped GB are shown in figure 3, figure 4 and figure 5 respectively. Energies are given relative to the Fermi level. The exchange splitting can be clearly seen. The small peaks appearing at about -7 eV and at about -5 eV are features relating to s and p states respectively. The contribution to the LDOS mainly comes from the d orbitals. It can be seen from figure 4 that the main LDOS peaks of Nb lie at energy positions lower than those of the neighbouring Fe2, Fe8 and Fe10 atoms, which means that the interaction of Nb with the neighbouring Fe atoms is weaker than that of Fe1 with the neighbouring Fe atoms, while for V-doped GB, the main LDOS peaks of V lie at almost the same energy positions as those of its neighbouring Fe atoms. Considering the different radial extents of 3d and 4d orbitals as well as their different energy positions, we can expect the bonding of Nb and the neighbouring Fe atoms to have some ionic-like components, while that between V and the neighbouring Fe atoms is still metallic-like. This agrees with the results on the charge distribution.
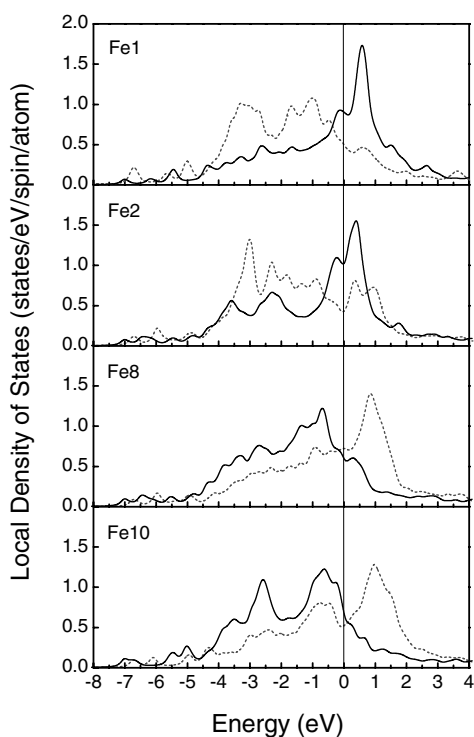
Figure 3. The LDOS curves for Fe1 and its neighbouring Fe2, Fe8 and Fe10 atoms in clean GB. The solid and dashed lines represent the spin-up states and the spin-down states respectively. The Fermi level is shifted to zero.
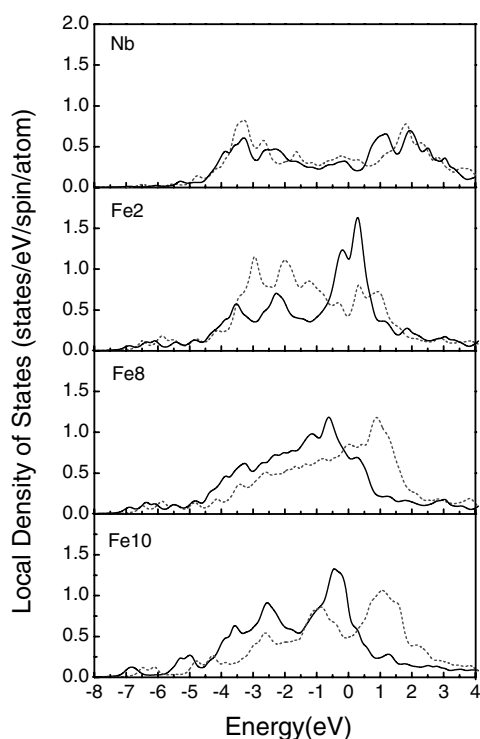
Figure 4. The LDOS curves for Nb and its neighbouring Fe2, Fe8 and Fe10 atoms in Nb-doped GB. The solid and dashed lines represent the spin-up states and the spin-down states respectively. The Fermi level is shifted to zero.
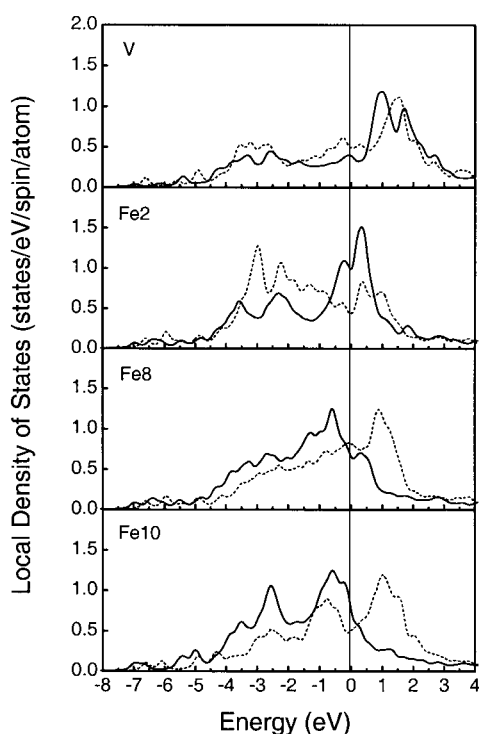
Figure 5. The LDOS curves for V and its neighbouring Fe2, Fe8 and Fe10 atoms in V-doped GB. The solid and dashed lines represent the spin-up states and the spin-down states respectively. The Fermi level is shifted to zero.

6. Summary

On the basis of the Rice–Wang thermodynamic model, we have studied the segregation effects of the alloying element Nb (V) on bcc $Fe\Sigma 3[1\bar{1}0](111)$ GB cohesion by the first-principles DMol method. The results show that the segregation of Nb (V) on the GB could improve the GB cohesion, which is beneficial as regards enhancement of the ductility of steel materials. We found that the chemical effect and the geometry effect of Nb and V play crucial but opposite roles in determining whether a material is brittle or ductile, and that the chemical effect is dominant and advantageous as regards grain boundary cohesion.

Acknowledgments

References

[1] Griffith A A 1920 *Phil. Trans. R. Soc.* A **200** 163
[2] Rice J R and Wang J S 1989 *Mater. Sci. Eng.* A **107** 23

[3] Tang S P, Freeman A J and Olson G B 1993 *Phys. Rev.* B **47** 2441
[4] Tang S P, Freeman A J and Olson G B 1994 *Phys. Rev.* B **50** 1
[5] Wu R, Freeman A J and Olson G B 1994 *Phys. Rev.* B **50** 75
[6] Wu R, Freeman A J and Olson G B 1994 *Science* **265** 376
[7] Wu R, Freeman A J and Olson G B 1996 *Phys. Rev.* B **53** 7504
[8] Zhong L, Wu R, Freeman A J and Olson G B 1997 *Phys. Rev.* B **55** 11 133
[9] Sagaert L P, Olson G B and Ellis D E 1998 *Phil. Mag.* B **77** 871
[10] Zhong L, Wu R, Freeman A J and Olson G B 2000 *Phys. Rev.* B **62** 13 938
[11] Feng Y and Wang C Y 2001 *Comput. Mater. Sci.* **20** 48
[12] Yang R, Zhao D L, Wang Y M, Wang S Q, Wang H Q, Ye H Q and Wang C Y 2001 *Acta Mater.* **49** 1079
[13] Delley B 1990 *J. Chem. Phys.* **92** 508
[14] Delley B 1991 *J. Chem. Phys.* **94** 7245
[15] Hohenberg P C and Kohn W 1964 *Phys. Rev.* **136** B864
[16] Kohn W and Sham L J 1965 *Phys. Rev.* **140** A1133
[17] Vosko S J, Wilk L and Nusair M 1980 *Can. J. Phys.* **58** 1200
[18] Allen M P and Tildesley D J 1987 *Computer Simulation of Liquids* (New York: Oxford University Press)
[19] Finnis M W and Sinclair J E 1984 *Phil. Mag.* A **50** 45
[20] Finnis M W and Sinclair J E 1986 *Phil. Mag.* A **53** 161
[21] Krasko G L and Olson G B 1991 *Solid State Commun.* **79** 113
[22] Mulliken R S 1955 *J. Chem. Phys.* **23** 1833